ACS Sustainable Chemistry & Engineering

Research Article

pubs.acs.org/journal/ascecg

Lignocellulose Fiber- and Welded Fiber- Supports for Palladium-Based Catalytic Hydrogenation: A Natural Fiber Welding Application for Water Treatment

David P. Durkin,[†] Tao Ye,[‡] Erik G. Larson,[§] Luke M. Haverhals,[§] Kenneth J. T. Livi,[∥] Hugh C. De Long,[⊥] Paul C. Trulove,[#] D. Howard Fairbrother,[†] and Danmeng Shuai*[,‡]

[†]Department of Chemistry, Johns Hopkins University, Baltimore, Maryland 21218, United States

[‡]Department of Civil and Environmental Engineering, The George Washington University, Washington, D.C. 20052, United States

[§]Department of Chemistry and Biochemistry, Bradley University, Peoria, Illinois 61625, United States

[∥]Department of Materials Science and Engineering, Johns Hopkins University, Baltimore, Maryland 21218, United States

[⊥]Air Force Office of Scientific Research, Arlington, Virginia 22203, United States

[#]Department of Chemistry, U.S. Naval Academy, Annapolis, Maryland 21401, United States

Supporting Information

ABSTRACT: In our study, lignocellulose yarns were fabricated via natural fiber welding (NFW) into a robust, free-standing, sustainable catalyst for water treatment. First, a series of powder catalysts were created by loading monometallic palladium (Pd) and bimetallic palladium−copper (Pd−Cu) nanoparticles onto ball-milled yarn powders via incipient wetness (IW) followed by a gentle reduction method in hydrogen gas that preserved the natural fiber while reducing the metal ions to their zerovalent state. Material characterization revealed Pd preferentially reduced near the surface whereas Cu distributed more uniformly throughout the supports. Although no chemical bonding interactions were observed between the metals and their supports, small (5−10 nm), near-spherical crystalline nanoparticles were produced, and a Pd−Cu alloy formed on the surface of the supports. Catalytic performance was evaluated for each Pd-only and Pd−Cu powder catalyst via nitrite and nitrate reduction tests, respectively. Next, the optimized Pd−Cu linen powder catalyst was fiber-welded onto a macroporous linen yarn scaffold via NFW and its catalyst performance and reusability were evaluated. This fiber-welded catalyst reduced nitrate as effectively as the corresponding powder, and remained stable during five consecutive cycles of nitrate reduction tests. Although catalytic activity declined after the fiber-welded catalyst was left in air for several months, its reactivity could easily be regenerated by thermal treatment. Our research highlights how lignocellulose supported metal-based catalysts can be used for water purification, demonstrating a novel application of NFW for water treatment while presenting a sustainable approach to fabricate functional materials from natural fibers.

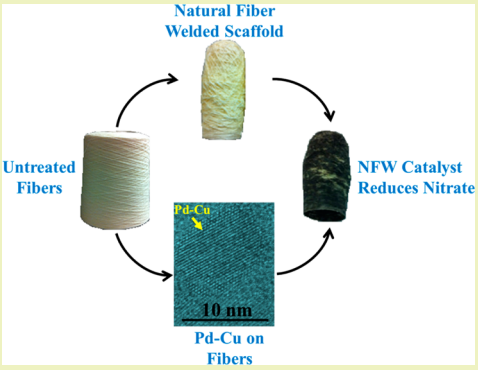

KEYWORDS: *Natural fiber welding, Lignocellulose, Ionic liquids, Catalyst, Palladium, Nitrate*

INTRODUCTION

Conventional catalyst supports with large surface areas, defined porous structures, and/or abundant surface functionality such as alumina,[1] silica,[2,3] titanium dioxide,[4] and activated carbon[5] have been extensively explored, as they promote uniform loading of metal nanoparticles with well-controlled properties to achieve decent catalytic performance. Emerging supports, such as carbon nanofibers,[6−8] carbon nanotubes,[9] and graphitic carbon nitride,[10,11] have received attention because they further improve catalytic performance. Because of limited postprocessing options, each of these supports is typically used as highly dispersed powders and are difficult to transport and recover. Additionally, manufacturing and recycling them can have a high negative environmental impact.[12,13] More sustainable supports and environmentally benign processing methods are needed to develop future catalysts.

Lignocellulose fibers represent a unique class of natural materials that hold great promise as catalyst supports, as they are earth-abundant, inexpensive, and rich in surface functional groups (e.g., −OH, −C−O−C−) that can promote nanoparticle deposition. Lignocellulose fibers consist primarily of cellulose, lignin, and hemicellulose.[14] Cellulose is a hydrophilic, crystalline, unbranched polysaccharide, with ca. 50 wt % oxygen, containing a well-defined structure of 6 hydroxyl groups (−OH) and 4 ether groups (−C−O−C−) per

Received: June 6, 2016
Revised: August 30, 2016
Published: September 12, 2016

DOI: 10.1021/acssuschemeng.6b01250
ACS Sustainable Chem. Eng. 2016, 4, 5511−5522

repeating unit. Lignin is a hydrophobic, amorphous, aromatic macromolecule with ca. 30 wt % oxygen.[15] Hemicellulose is an amorphous, branched polysaccharide that cross-links cellulose microfibrils together through hydrogen bonding. The structures of lignin and hemicellulose vary with plant species, and the contents of cellulose, lignin, and hemicellulose in lignocellulose fibers also vary with plant species, plant age, and postprocessing. For example, processing flax into linen yarn removes the majority of lignin and fillers,[16] leaving a material approximately 80 wt % cellulose and 2−5 wt % lignin.[14,17,18] In contrast, processed bamboo fibers have more lignin (ca. 20−32 wt %) and less cellulose (ca. 40−60 wt %).[17,19] Different cellulose and lignin contents may lead to distinct behaviors in catalyst preparation and subsequent performance. Hydrophilic linen may promote uniform catalytic metal loading and reduced metal nanoparticle size because of increased interaction with metal precursors, whereas bamboo fibers with a higher lignin content are more hydrophobic and may be more resistant to thermal decomposition in catalyst fabrication.[18,20,21]

Previous studies have demonstrated that lignocellulose can support the uniform loading of catalytic metals. For example, Quignard et al. prepared catalysts on cellulose powder to catalyze an allylic substitution reaction.[22] He et al. reported a noble-metal nanoparticle synthesis in cellulose paper, investigating how the cellulose ether and hydroxyl functional groups facilitate the growth of extremely small nanoparticles.[23] Reddy et al. prepared Pd catalysts in cellulose powders to facilitate the Heck and Sonagashira coupling reaction.[24] Padalkar et al. developed nanofabrication techniques to control and optimize monometallic nanoparticle deposition onto cellulose nanocrystals.[25]

A distinct advantage of lignocellulose over conventional catalyst supports is that it can be postprocessed through natural fiber welding (NFW)[26] into free-standing structures. In NFW, lignocellulose fibers are partially dissolved and mobilized upon exposure to controlled amounts of ionic liquid (IL), then reorganized upon IL removal.[27] The NFW process is environmentally benign and sustainable because ILs can be recycled. Moreover, ILs can be derived from biomass, further enhancing NFW's sustainability potential.[28] NFW is quite versatile, as any number of ILs can be applied to natural fiber materials including lignocellulose (e.g., cotton, linen, hemp, bamboo) and other biopolymers (e.g., silk, chitin). Additionally, studies have shown that NFW can maintain or improve the mechanical properties of the underlying natural fiber supports,[27,29−32] extending their use to more advanced engineering applications. In previous work, researchers at the U.S. Naval Academy and Bradley University have used NFW to modify natural fibers with functional materials, e.g., conductive carbons[33] or fluorescent dyes.[27] In this study, we developed lignocellulose fibers as supports for Pd-based catalysts, and then demonstrated how NFW can transform them into a catalytic free-standing structure for water purification of nitrate. To the best of our knowledge, no lignocellulose fiber-welded catalysts have been developed to date.

Nitrate is a persistent contaminant in groundwater and surface water,[34] generated from extensive agricultural practices, industrial processes, and improper septic disposal,[35−37] and can lead to "blue baby syndrome".[38] Nitrite is a reduction intermediate of nitrate, and can be converted *in vivo* to *N*-nitroso compounds, which are known carcinogens.[39,40] Because of these health concerns, the World Health Organization (WHO) and U.S. Environmental Protection Agency (USEPA) have recommended maximum contaminant levels for nitrate and nitrite in drinking water: 50 mg L^{-1} for nitrate by the WHO,[41] 10 and 1 mg L^{-1} as N for nitrate and nitrite by the USEPA.[42] Noble-metal-based catalytic hydrogenation has emerged as a promising strategy to reduce waterborne nitrate and nitrite, according to the reaction in Scheme 1.[43−46]

Scheme 1. Nitrate Reduction Pathway on Noble-Metal-Based Catalysts, with *NO* as a Proposed Intermediate

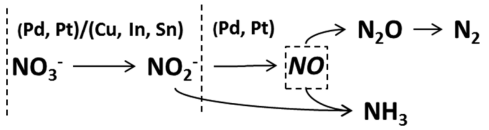

Nitrate reduction to nitrite requires a noble metal (e.g., Pd, Pt) in close proximity or direct contact with a promoter metal (e.g., Cu, In, Sn), whereas the reduction of nitrite and other intermediates (e.g., N_2O) only requires the noble metal. The noble metal dissociates hydrogen gas to facilitate both reductions.[47] Compared to other bimetal catalysts, Pd−Cu holds promise for nitrate reduction in water treatment because of its fast reduction kinetics and selectivity toward dinitrogen gas vice ammonia, an undesirable byproduct for drinking water.[46,48−50]

In the present investigation, initial experiments loading Pd and Cu directly onto linen and bamboo yarns via impregnation methods were successful; however, it was difficult to control catalyst loading and to disperse the yarns in solution to test catalytic performance. To overcome these challenges, we milled the lignocellulose yarns to powder, and then used incipient wetness (IW) to deposit metal ions from aqueous solution into the fibers. Subsequent heat treatment of the impregnated powders in N_2 and H_2 at low temperature (120 °C) deposited very small metal nanoparticles (ca. 5−10 nm) throughout the support while maintaining the integrity of the fibers. Mass loadings of Pd and Cu were tailored to optimize catalytic performance toward nitrite and nitrate reduction. Through a suite of characterization techniques, we explored the material's surface and bulk chemistry to understand relationships between catalyst properties and reactivity.

By maintaining the integrity of the natural fiber support during nanoparticle synthesis, the catalyst powder could subsequently be used in an NFW application. We first used NFW to create a macroporous linen scaffold. Then we fiber-welded the most reactive bimetal catalyst powder onto the scaffold surface, and used this free-standing structure to reduce nitrate. Reactivity testing revealed a robust, sustainable, catalytic structure that can be used over multiple reaction cycles, and that can be regenerated to full catalytic performance with a simple, low temperature tube furnace treatment under N_2 and H_2 at 105 °C. This is the first report to develop Pd-based catalysts on lignocellulose supports for water purification, and the first study that demonstrates the fabrication and application of NFW catalysts. More importantly, these sustainable methods can be applied generally to create a myriad of lignocellulose-supported nanoparticle systems, and to fabricate them into advanced functional materials.

EXPERIMENTAL SECTION

Materials Preparation. A full description of chemicals, materials, and methods is provided in the Supporting Information (SI). Each chemical or material was used as received. Yarns of linen (L) and

DOI: 10.1021/acssuschemeng.6b01250
ACS Sustainable Chem. Eng. 2016, 4, 5511−5522

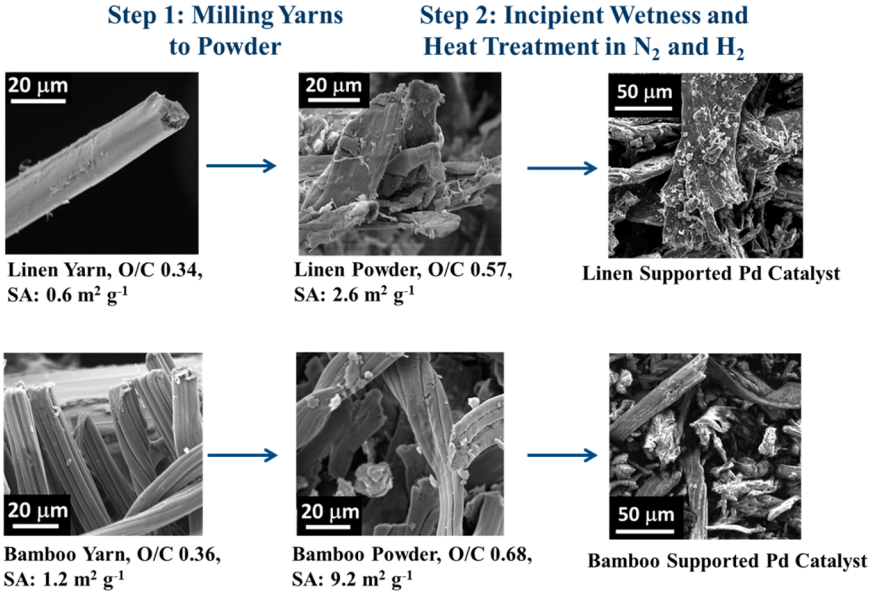

Figure 1. Development of lignocellulose yarns into Pd-based catalysts. Scanning electron microscopy (SEM) images were acquired at 10 kV. O/C is the surface oxygen to carbon atomic ratio measured by X-ray photoelectron spectroscopy (XPS). The surface area (SA) of untreated fibers was measured by liquid N_2 adsorption.

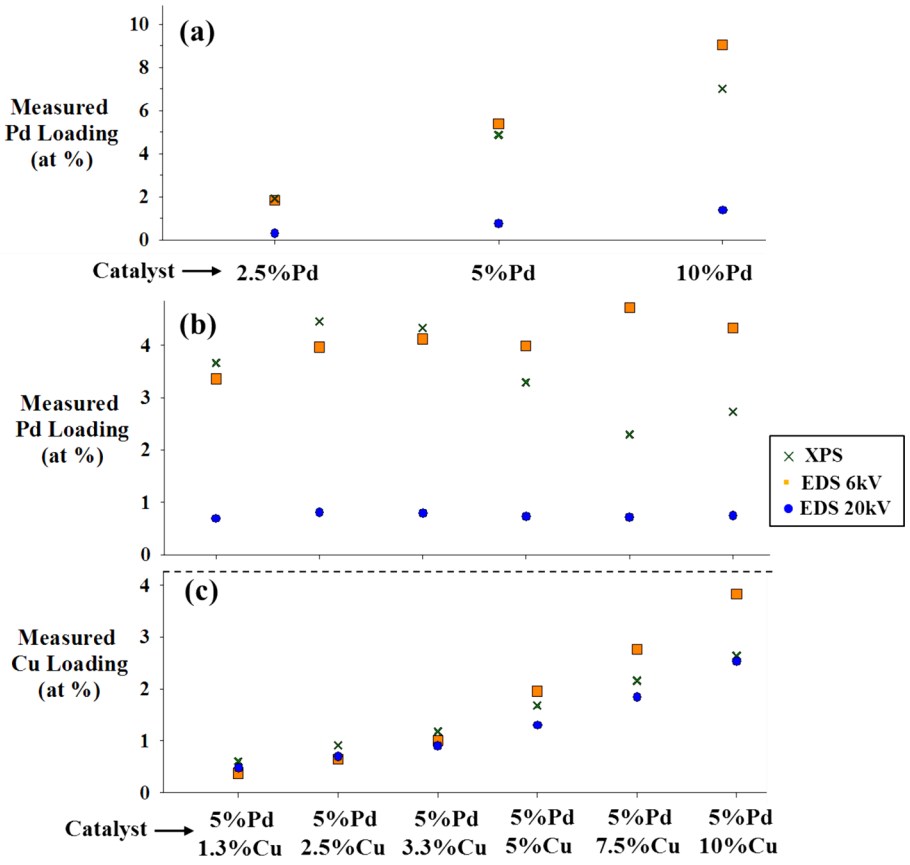

Figure 2. X-ray photoelectron spectroscopy (XPS) and energy-dispersive X-ray spectroscopy (EDS) elemental analyses of Pd-based catalysts supported on linen powder. (a) Pd loadings of Pd-only catalysts; (b) Pd loadings of Pd−Cu catalysts; (c) Cu loadings of Pd−Cu catalysts. For each catalyst, the *x*-axis shows the theoretical mass loadings of metals, represented by weight percentage. Panels b and c share a common *x*-axis.

bamboo (B) were milled using a FlackTek shear mixer (AM-601). Pd and Pd−Cu were loaded onto linen and bamboo powder by incipient wetness (IW). This process involves impregnating the powders with aqueous, metal nitrate solutions whose volume equaled the pore volume of the powder, the latter determined by mass difference between dry and water-saturated fibers. Metal loadings were varied by adjusting the metal concentrations in solution. Following IW, the powders were air-dried, and then sequentially heated under N_2 and H_2 (120 °C for 2 h in each gas) to reduce the salts and produce metal nanoparticles.

DOI: 10.1021/acssuschemeng.6b01250
ACS Sustainable Chem. Eng. 2016, 4, 5511−5522

The following catalyst label code was used: "Substrate_wt %Pdwt % Cu". Theoretical mass loadings of metals were reported in the code. For example, bamboo powder (B) with 5 wt % Pd was labeled B_5Pd. Linen powder (L) with 5 wt % Pd and 1.3 wt % Cu was labeled L_5Pd1.3Cu. Untreated linen and bamboo yarns were labeled L_Y and B_Y, respectively.

For the NFW process, a tubular linen support was first prepared from partial dissolution and reconstitution of linen yarn in an IL, 1-ethyl-3-methyl imidazolium acetate (EMI-Ac), based on previously reported methods.[26] Next, a certain amount of linen-supported Pd−Cu catalyst was dissolved with EMI-Ac and acetonitrile, and the resulting "catalytic ink" was fiber-welded onto the tubular linen support under vacuum at 60 °C.

Materials Characterization. Full details of the materials characterization methods are provided in the SI. Inductively coupled plasma-mass spectrometry (ICP-MS) (Agilent 7500) evaluated mass loadings of Pd and Cu; X-ray photoelectron spectroscopy (XPS) identified the oxidation states of Pd, Cu, and C, and surface concentrations of Pd, Cu, C, and O; attenuated total reflection-Fourier transform infrared spectroscopy (ATR-FTIR) (Nicolet iS10) probed the functional groups in the linen and bamboo supports; scanning electron microscopy/energy dispersive X-ray spectroscopy (SEM/EDS) (TESCAN MIRA3, TEAM Octane SSD) examined the catalyst morphology, catalyst composition, and distribution of metals throughout the support and fiber-welded catalyst; transmission electron microscopy (TEM) (Philips CM300 FEG) evaluated the morphology, composition, and crystal structure of metal nanoparticles; liquid N_2 adsorption (Micromeritics Tristar 3000 Gas Adsorption Analyzer) determined surface area via the Brunauer−Emmett−Teller (BET) method.

Catalytic Reduction Tests. To investigate catalytic performance toward contaminant removal, powdered catalysts were dispersed, and the welded-fiber catalyst was fully submerged, in a phosphate buffer (pH 7.3, 1 mM). The catalyst and buffer were presparged with hydrogen gas to recondition metals that may have oxidized during storage.[7] During reduction tests, hydrogen gas flow of 150 mL min^{-1} supplied sufficient reductant and solutions were mixed at 500 rpm to eliminate mass transfer limitations.[7] Evaluation of mass transfer rates (see the SI) indicated both aqueous/solid and intraparticle mass transfer did not influence the measured reactivity. During reduction tests, contaminant concentrations were determined at regular time intervals by ion chromatography (Dionex ICS-1100). After a prolonged period of storage in ambient conditions the welded-fiber catalyst was regenerated by heat treatment under N_2 and H_2 at 105 °C (2 h in each gas) for multiple cycles of nitrate reduction tests. Further experimental details are provided in the SI.

RESULTS

Catalyst Supports Created from Linen and Bamboo Yarns. To prepare catalyst supports successfully from lignocellulose yarns, it was necessary to mill the yarns to a powder before metal deposition. The SEM images in Figure 1 depict the morphology of untreated lignocellulose yarns, ball-milled yarn powders, and catalytic metal-loaded powders. As supplied, both linen and bamboo yarns were composed of microfiber bundles (diameter ca. 10−15 μm). Both yarns fractured significantly upon milling but kept their fibrous structure. XPS revealed that milling increased the surface atomic oxygen to carbon (O/C) ratio of each support (i.e., linen O/C increased from 0.34 to 0.57; bamboo O/C increased from 0.36 to 0.68). Milling also increased the support surface area (SA) (i.e., linen SA increased from 0.6 to 2.6 m^2 g^{-1}; bamboo SA increased from 1.2 to 9.2 m^2 g^{-1}). After metal loading, the SEM images (right side of Figure 1) revealed that the fibrous structure of the yarns remained intact, with metal particles (confirmed by EDS elemental mapping, not shown) dispersed throughout the matrix.

Catalyst Composition and Metal−Support Interaction. Bulk and surface elemental analyses for all catalysts was accomplished using ICP-MS, XPS, and EDS (Figures 2, S1−3). The ICP-MS data are reported as weight percentage (wt %) of total catalyst, and compared with theoretical metal loadings determined from the mass of ions used in IW. Both XPS and EDS data are reported as atomic percentage (at. %).

Table S1 shows results on the loading of Pd and Cu, determined by ICP-MS of acid digested catalyst powders. These data are generally close to the theoretical metal loadings, indicating IW was an effective method to load the metals onto the supports. The data also indicate that IW was more efficient in loading metals onto linen than on bamboo.

XPS measured the amount of Pd and Cu near the support surface (<ca. 10 nm) (Figures 2 and S1). To complement the XPS analyses, EDS data acquired as a function of incident electron energy was used to semiquantitatively determine Pd and Cu content from the near-surface region (ca. 500 nm) and into the bulk (up to several μm). The effective interaction volume and penetration depth of the electron beam used in EDS were determined through a Monte Carlo simulation.[51] Assuming the density of cellulose, this simulation revealed that as the acceleration voltage increased from 6 to 30 kV, the beam penetration depth increased from ca. 500 nm to 9.5 μm, whereas the electron beam interaction volume increased exponentially from ca. 0.1 to 800 μm^3. Data acquired at low (6 kV) and high (20 kV) acceleration voltages therefore afforded a comparison between elemental compositions in the near-surface region and volumes more representative of the bulk.

Figure 2 summarizes the XPS and EDS data acquired for each catalyst prepared on linen. Analogous data for bamboo catalysts is presented in Figure S1. For each plot, the *x*-axis lists the material tested, and the *y*-axis presents the corresponding chemical composition determined by XPS and EDS, the latter acquired at 6 kV and 20 kV. Paired *t* tests revealed that the EDS data acquired at 6 kV and the XPS data for both Pd and Cu were statistically similar ($p > 0.05$). For Cu, the XPS data remained statistically correlated with EDS data obtained through 20 kV. In contrast, this correlation did not hold for Pd; at each acceleration voltage above 6 kV the Pd data measured by EDS were lower than the XPS data, approaching bulk Pd loadings at 20 kV. For each catalyst studied, the Pd concentrations determined by EDS decreased exponentially (R^2 = 0.86−0.93) as the acceleration voltage increased (see Figures S2−3). By 20 kV, the Monte Carlo simulation suggests that the electron beam probed a depth of ca. 5 μm, nearly halfway through a microfiber bundle. Interestingly, at this probe depth, the measured Pd and Cu loadings most closely approximate the theoretical loadings. Combined, the XPS and EDS data indicated that Pd reduced preferentially in the near surface regions (surface to ca. 500 nm) for all catalyst systems. Conversely, Cu was more uniformly distributed throughout natural fiber supports.

Infrared spectroscopy of the yarns and milled yarn powders (Figure S4) showed dominant absorption bands characteristic of lignocellulose: O−H stretching (3600−3000 cm^{-1}), C−H stretching (ca. 2950 cm^{-1}), and C−O stretching (ca. 1020 cm^{-1}).[52] A comparison of ATR-FTIR spectra before and after metal loading showed no shifting or significant changes in these regions. The ATR-FTIR analyses not only verified that the support remained lignocellulose in nature after the initial thermal treatment and the metal deposition process but also

DOI: 10.1021/acssuschemeng.6b01250
ACS Sustainable Chem. Eng. 2016, 4, 5511−5522

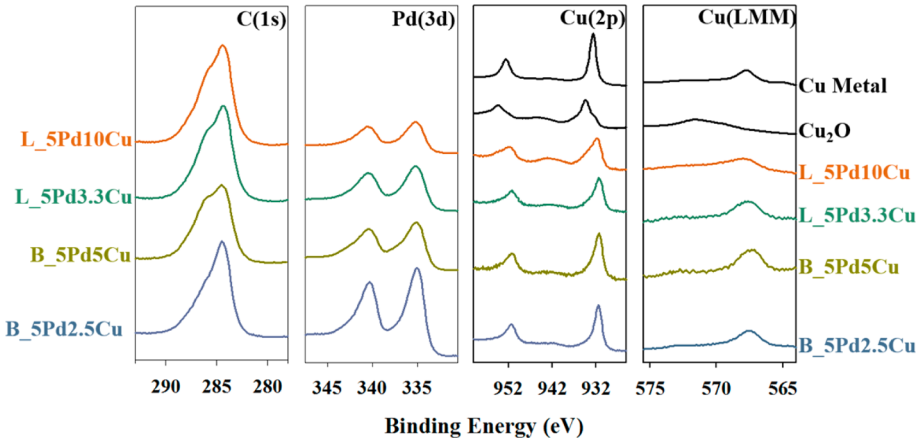

Figure 3. Representative X-ray photoelectron spectroscopy (XPS) of Pd−Cu catalysts supported on linen (L) and bamboo (B) powder. Spectra for copper metal and Cu_2O are also included as references to aid in Cu(0) and Cu(I) identification. Catalyst label code was "Substrate_wt %Pdwt %Cu". The theoretical mass loadings of metals, represented by weight percentage, were reported in the code.

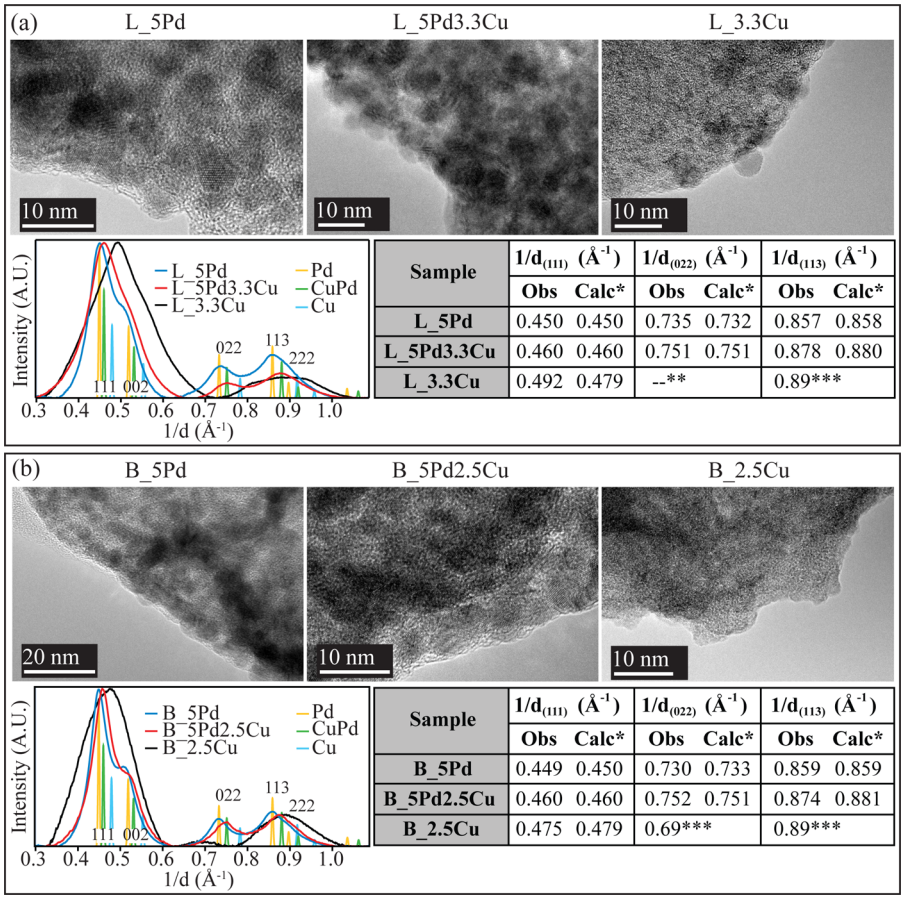

Sample	$1/d_{(111)}$ (Å^{-1})		$1/d_{(022)}$ (Å^{-1})		$1/d_{(113)}$ (Å^{-1})	
	Obs	Calc*	Obs	Calc*	Obs	Calc*
L_5Pd	0.450	0.450	0.735	0.732	0.857	0.858
L_5Pd3.3Cu	0.460	0.460	0.751	0.751	0.878	0.880
L_3.3Cu	0.492	0.479	--**		0.89***	

Sample	$1/d_{(111)}$ (Å^{-1})		$1/d_{(022)}$ (Å^{-1})		$1/d_{(113)}$ (Å^{-1})	
	Obs	Calc*	Obs	Calc*	Obs	Calc*
B_5Pd	0.449	0.450	0.730	0.733	0.859	0.859
B_5Pd2.5Cu	0.460	0.460	0.752	0.751	0.874	0.881
B_2.5Cu	0.475	0.479	0.69***		0.89***	

Figure 4. Transmission electron microscopy (TEM) of linen (L, panel a) and bamboo (B, panel b) powder catalysts with Pd, Pd−Cu, and Cu deposited *in situ*. High resolution TEM (HRTEM) images are presented for each system, along with radially averaged selected area electron diffraction (SAED) profiles of dispersed nanoparticles. The centroid peak positions measured in each sample are referenced to the Inorganic Crystal Structures Database (ICSD). Catalyst label code was "Substrate_wt %Pdwt %Cu". The theoretical mass loadings of metals, represented by weight percentage, were reported in the code.

revealed that the metal atoms did not form strong chemical interactions with the functional groups of the lignocellulose.

Chemical Characterization of Metal Nanoparticles. XPS was also used to characterize the bonding environment and oxidation state of the catalysts (Figures 3, S5−6). Figure 3 shows the Pd(3d), Cu(2p), and C(1s) regions for representative Pd−Cu linen and bamboo catalysts with a fixed Pd loading (5 wt %, theoretical) and various Cu loadings. Irrespective of Cu loading, there was a Pd($3d_{5/2}$/$3d_{3/2}$) doublet in the Pd(3d) region consistent with the presence of a single species; the Pd($3d_{5/2}$) binding energy was located at 335.0 eV (±0.2 eV), indicative of metallic Pd.[53] In some Pd(3d) spectra, a slight shoulder on the higher binding energy side of the Pd($3d_{5/2}$/$3d_{3/2}$) doublet was observed, indicating a small amount of

DOI: 10.1021/acssuschemeng.6b01250
ACS Sustainable Chem. Eng. 2016, 4, 5511−5522

oxidized Pd was present, most likely from unreduced Pd^{2+} adsorbed on the surface.

Analysis of the Cu(2p) region indicated two peaks consistent with a Cu($2p_{3/2}$/$2p_{1/2}$) doublet, whose Cu $2p_{3/2}$ peak position (931.4 ± 0.2 eV) could be from either Cu(0) or Cu(I) species; distinguishing the oxidation state of Cu atoms requires inspection of both the Cu(2p) XP transition and the Cu(LMM) Auger lineshapes.[54,55] By comparing the Cu(2p) and Cu(LMM) of the Pd−Cu catalysts to reference spectra of Cu(0) and Cu(I) species obtained in the same instrument, Figure 3 shows that the Cu was present as Cu(0). XPS analyses of two additional samples prepared with Cu but no Pd (Figure S6) showed Cu present only as Cu(II) and Cu(I), confirming that Pd was required along with hydrogen to reduce the Cu ions effectively to the zerovalent state. For one catalyst (L_5Pd10Cu), the appearance of a higher binding energy shoulder in the Cu($2p_{3/2}$/$2p_{1/2}$) doublet, along with a distinct shakeup feature at 943 eV, indicated the presence of some Cu(II) species in that sample. Thus, for the highest Cu loading, some Cu did not get reduced during catalyst preparation, or possibly some Cu was air-oxidized during storage.

Two primary carbon species were observed in the C(1s) region for every catalyst. The lower C(1s) binding energy region (284.5 eV) was attributed to alkyl carbon (i.e., −C−C− or −C−H), an expected carbon species in the lignocellulose supports. The higher binding energy region (>286 eV) was attributed to higher oxidation state carbon singly bonded to oxygen (i.e., the C−OH and −C−O−C), also expected for lignocellulose supports.[56] The XPS spectra of untreated yarns and powders (Figure S5) indicated that milling exposed a higher concentration of this higher oxidation state carbon at the support surface. Upon metal deposition/catalyst preparation, no significant shifts or new peaks were observed in the C(1s) envelopes, supporting the earlier conclusion (from ATR-FTIR) that the metals did not form chemical bonds with the oxygen-containing functional groups in either the linen or bamboo supports.

TEM Characterization of Lignocellulose Catalysts. Samples with only Pd or Cu loaded on linen and bamboo, along with the two most reactive bimetal catalysts (L_5Pd3.3Cu and B_5Pd2.5Cu) were investigated with TEM to assess metal nanoparticle size, distribution, and structure. The Cu-only samples were prepared to compare their selected area electron diffraction (SAED) profiles with those acquired from the Pd and Pd−Cu catalysts.

High-resolution TEM (HRTEM) images of fiber edges from the six samples are presented in Figure 4. The L_5Pd, B_5Pd, and both bimetal catalysts all contained near-spherical nanoparticles with sizes around 5−10 nm. All nanoparticles clearly showed lattice fringes, indicating they were crystalline. The L_3.3Cu sample contained a lower density of crystalline Cu nanoparticles, whereas none could be detected in B_2.5Cu.

SAED patterns from areas ca. 5 μm in diameter acquired from the fiber edges of the catalysts are presented in Figure 4. For B_5Pd2.5Cu and L_5Pd3.3Cu, measured reflections at (111), (022), and (113) closely correlate with the calculated values for Pd−Cu alloy, referenced to the Inorganic Crystal Structures Database (ICSD). These results agree with previous observations that Pd and Cu readily form alloys.[57−59] The SAED patterns for the Pd-only catalysts clearly correlate with Pd referenced from the ICSD. The (111) and (002) peaks for B_5Pd and B_5Pd2.5Cu are sharper than those for L_5Pd and L_5Pd3.3Cu, indicating that metal nanoparticles on bamboo are larger and more crystalline than those on linen. Because of the small nature of the nanoparticles and the crystallinity of the lignocellulose support, the peaks at (002) and (222) could not be resolved.

EDS spectra (Figure S7) taken on the outer edges of the fibers for each of the six samples show that the expected elements are present. The Mo L peak found in all spectra originated from the Mo support grid. The Cu Kα peak in the L_5Pd sample originates from X-ray fluorescence of the brass holder and is found in every spectrum even where no Cu was added. The EDS analyses show that Pd dominates over Cu at the outer edge of the fibers. This is consistent with the elemental analyses acquired by SEM/EDS and XPS. The ratio of Pd to Cu varies greatly in different areas, and some pure Cu crystals were found in both bimetallic catalysts.

Nitrite and Nitrate Reduction on Pd-Based Linen and Bamboo Powder Catalysts. Each Pd-only catalyst was assessed in nitrite reduction tests (Figure 5a) to determine the impact of metal loading on catalytic performance. Nitrite reduction rate constants are reported as a function of Pd loading (wt %), the latter measured by ICP-MS (Table S1). For the linen-supported Pd catalysts, nitrite reduction activity was linearly related (R^2 = 0.88) to Pd loading across the range

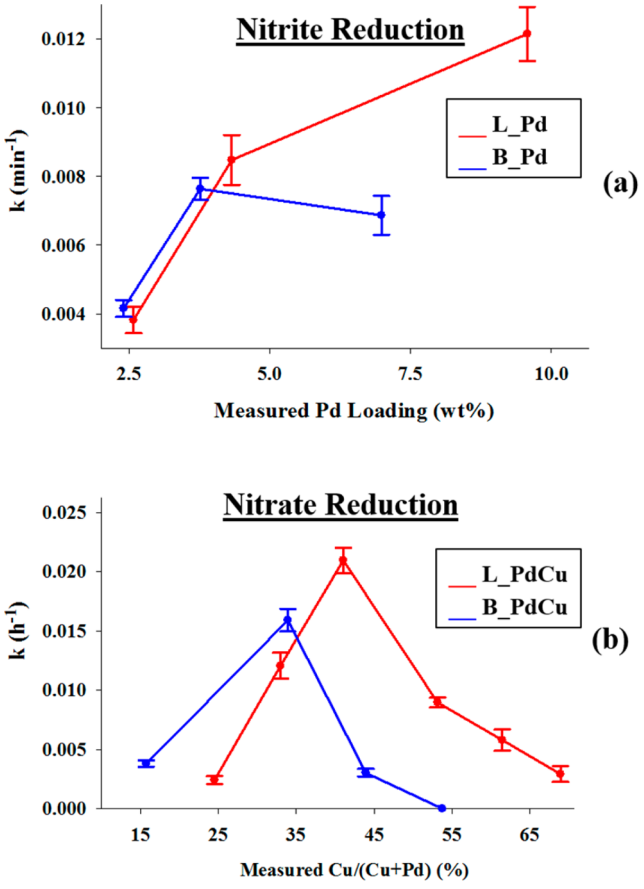

Figure 5. Nitrite and nitrate reduction kinetics (reported as pseudo-first-order rate constants) of linen powder (L) and bamboo powder (B) supported Pd-based catalysts. In Figure 5b the Pd loading is reported as the mass of Pd to total mass of catalyst; the Cu/(Cu+Pd) percentage represents the mass of Cu to Cu plus Pd. Both metal loadings were determined by inductively coupled plasma-mass spectrometry (ICP-MS). Catalyst label code was "Substrate_Pd" and "Substrate_PdCu" for Pd-only and Pd−Cu catalysts, respectively.

DOI: 10.1021/acssuschemeng.6b01250
ACS Sustainable Chem. Eng. 2016, 4, 5511−5522

studied (2.6−9.6 wt %, ICP-MS). For the bamboo-supported Pd catalysts, reactivity first increased proportionally with the Pd loading (2.4−3.8 wt %, ICP-MS), then leveled off as Pd loading increased further (3.8−7.0 wt %, ICP-MS).

Each Pd−Cu catalyst was assessed in nitrate reduction tests (Figure 5b) to determine the impact of Cu composition on catalytic performance. The Pd−Cu catalysts were prepared with the theoretical Pd loading of 5 wt %, and varied theoretical Cu loadings from 1.3 to 10 wt % (on linen) and 1.3−5 wt % (on bamboo). Nitrate reduction rate constants are reported as a function of the Cu/(Cu+Pd) percentages (wt %) measured by ICP-MS (Table S1). The measured Cu/(Cu+Pd) percentages ranged from 25 to 69% (linen) and 16−54% (bamboo), as shown in Figure 5b.

For the linen-supported Pd−Cu catalysts, as Cu/(Cu+Pd) increased from 25 to 41%, nitrate reduction rate constants increased by almost an order of magnitude, from 2.4(±0.3) × 10^{-3} to 2.1(±0.1) × 10^{-2} h^{-1}. However, at higher Cu loadings, the nitrate reduction rate constant decreased steadily until it reached 2.9(±0.7) × 10^{-3} h^{-1} when the Cu/(Cu+Pd) percentage was 69%. When the Cu/(Cu+Pd) percentage exceeded 69%, the fibers decomposed into a caramelized char during heat treatment, and were not used for the reactivity study.

The effect of loading Cu and Pd on bamboo produced a qualitatively similar trend with the presence of an optimal Cu loading. As the Cu/(Cu+Pd) percentage in the bamboo bimetallic catalysts increased from 16 to 34%, nitrate reduction rate constants increased from 3.8(±0.3) × 10^{-3} to 1.6(±0.1) × 10^{-2} h^{-1}. Further increases in Cu/(Cu+Pd) percentage resulted in lower reactivity, with the rate constants decreasing significantly when the Cu/(Cu+Pd) percentage reached 54%. The optimized bamboo catalyst (B_5Pd2.5Cu, k = 1.6(±0.1) × 10^{-2} h^{-1}) was only slightly less reactive than the optimized linen bimetal catalyst (L_5Pd3.3Cu, k = 2.1(±0.1) × 10^{-2} h^{-1}). Although B_5Pd5Cu showed no measurable reactivity, it did not decompose during synthesis and was therefore still characterized.

Table S2 compares the performance of the lignocellulose-supported Pd and Pd−Cu with similar catalysts on other conventional supports (i.e., activated carbon, TiO_2, alumina, silica). This comparison shows that the lignocellulose-supported Pd-based catalysts have comparable performance. Differences are expected due to the varied nature of each support and widely varied testing conditions (i.e., pH, buffer, initial concentration of contaminant, catalyst loading) used in each study.

Nitrate Reduction with a Fiber-Welded Pd−Cu Catalyst Reactor. The most reactive powdered catalyst (L_5Pd3.3Cu) was selected as the active component in the NFW "ink" to develop the fiber-welded catalyst reactor. Preserving the lignocellulose fibers during metal deposition process was critical, as it ensured the powder could be used in this NFW application.

First, untreated linen yarn was transformed via NFW into the desired shape for the catalyst scaffold (Figure 6), forming a rigid, macroporous support onto which the powder catalyst would be loaded. A batch of L_5Pd3.3Cu (mass of 2 g) was prepared for use as the raw material to weld to the free-standing linen scaffold. Some of this catalyst powder was solubilized with IL into a catalyst "ink", and welded onto the surface of the linen scaffold through NFW (Figure 6). The fiber-welded catalyst was significantly mechanically stronger than the native linen

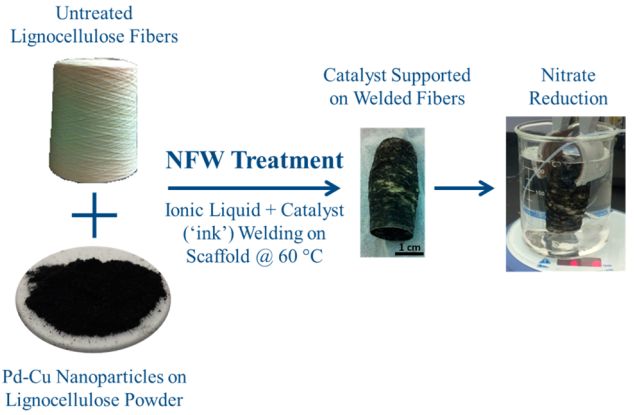

Figure 6. Natural fiber welding of Pd−Cu catalyst powder onto linen yarn support.

yarns, an expected benefit of the NFW process.[26,29] SEM and EDS mapping were used characterize the fiber-welded catalyst (Figure S8). These SEM images show that the catalyst is welded on the surface of the linen scaffold, and EDS of several areas ca. 500 μm in diameter confirmed the Cu/(Cu+Pd) composition was 40(±2) wt %, as expected (Figure S8a). Elemental mapping of this interface (Figure S8b) clearly showed that Pd and Cu were well-distributed on the scaffold surface during welding.

The fiber-welded catalyst and its constituent powder were evaluated in nitrate reduction tests (Figure 7a). After normalizing to catalyst loading, the nitrate reduction rate constants for the powdered catalyst and the fiber-welded catalyst were 2.2(±0.2) × 10^{-2} L (g of catalyst)$^{-1}$ h^{-1} and 2.2(±0.05) × 10^{-2} L (g of catalyst)$^{-1}$ h^{-1}, respectively. This reactivity was lower than expected for L_5Pd3.3Cu, as reported in Figure 5 (i.e., 4.2(±0.2) × 10^{-2} L (g of catalyst)$^{-1}$ h^{-1}). Through NFW, the functional material was also immobilized within a robust, sustainable natural fiber framework, enabling catalytic reduction of water contaminants, as well as easy recovery and reuse of the catalyst after the reaction. The test solution was analyzed via ICP-MS for dissolved Pd and Cu after catalytic reaction, and the results indicated less than 0.6% of Pd and less than 0.5% of Cu leached from the NFW structure during nitrate reduction.

After testing, the fiber-welded catalyst was exposed to air under an ambient condition for 4 months and the reactivity was completely lost. Hydrogen sparging at room temperature failed to regenerate the fiber-welded catalyst, and it was unreactive during a second nitrate test (Figure 7b). However, heating the fiber-welded catalyst at 105 °C under N_2 and H_2 gas restored its reactivity to 4.5(±0.3) × 10^{-2} L (g of catalyst)$^{-1}$ h^{-1}. After regeneration, the fiber-welded Pd−Cu catalyst underwent 70 h of multiple nitrate reduction tests over 5 days (Figure 7b), exhibiting good stability during each test and reproducibility with an average nitrate rate constant of 4.1(±0.2) × 10^{-2} L (g of catalyst)$^{-1}$ h^{-1}. Between each 14-h test, the reactor was removed from the test solution, rinsed with water, and stored at 60 °C in air. Following a second regeneration, no significant changes to reactivity were observed in a final test of the system.

DISCUSSION

Viability of Lignocellulosic Fibers as Catalyst Supports. Thermal decomposition of cellulose begins above 150 °C,[14] and Cu is a known catalyst for facilitating cellulose

DOI: 10.1021/acssuschemeng.6b01250
ACS Sustainable Chem. Eng. 2016, 4, 5511−5522

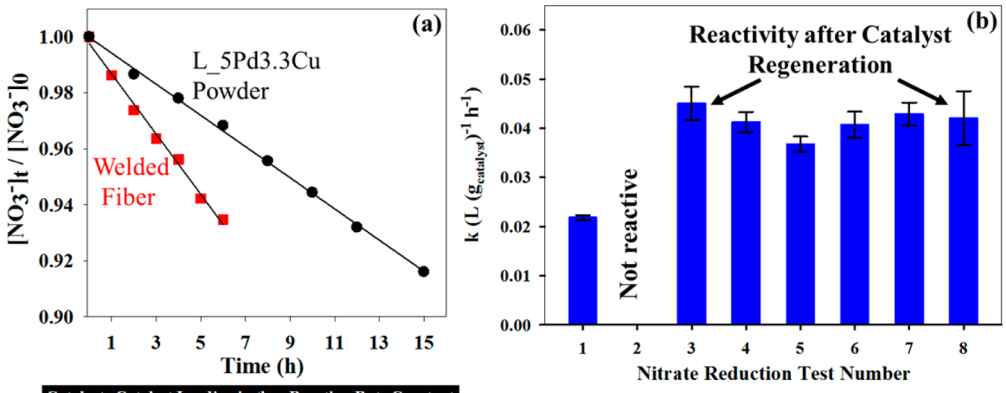

Catalyst	Catalyst Loading in the Reaction Solution (g L^{-1})	Reaction Rate Constant (L g^{-1} h^{-1})
Powder	0.5	2.2(± 0.2) x 10^{-2}
Welded Fiber	0.265	2.2(± 0.05) x 10^{-2}

Figure 7. Nitrate reduction kinetics for (a) the welded-fiber catalyst and its comparison with the powdered catalyst, and (b) the welded-fiber catalyst during 114 h of nitrate reduction tests. (Test 1) Initial nitrate reduction test, as described in panel a. (Test 2) No reactivity was observed following sparging catalyst with H_2 at room temperature, after the catalyst being stored in air at room temperature for 4 months. (Test 3) Catalyst performance restored after heat treatment of 105 °C under N_2 and H_2, each for 2 h, respectively. (Tests 3−7) Catalyst reduced nitrate for 14 h per day for 5 consecutive days. Between tests 3−7, the catalyst was rinsed with water and stored at 60 °C in air. (Test 8) Catalyst performance following a second regeneration with N_2 and H_2 at 105 °C, each for 2 h, respectively. Pseudo-first-order rate constants are normalized to catalyst loading, calculated as the mass of catalyst in the total volume of reaction solution. Catalyst label code L_5Pd3.3Cu represents linen powder supporting 5 wt % of Pd and 3.3 wt % of Cu, with theoretical loadings of both metals reported.

thermal degradation.[60] We conducted a series of preliminary experiments to investigate the thermal stability of cotton, linen, and bamboo yarns and to assess the viability of lignocellulosic fibers as catalyst supports. Results from these studies revealed that (i) bamboo and linen were more thermally stable than cotton (i.e., only cotton fibers decomposed to char), (ii) 120 °C was the highest temperature that could be used to reduce Cu and Pd in hydrogen gas without altering the lignocellulose nature (i.e., at higher temperatures, all fibers decomposed to char), and (iii) milling fibers to powder before metal deposition improved the ability to control metal loading.

The changes in surface O/C atomic ratio and surface areas after milling correlate with a recent study by Csiszar et al.[56] who showed that milling linen fibers increases the surface O/C atomic ratio by exposing the more oxygen-rich carbon moieties of cellulose. Moreover, milling can increase the fibers water sorption capacity while exposing some underlying microfibril structure.[56] These physical and chemical changes promoted uniform loading of catalytic metals and dispersion of the powdered catalysts in solution, enabling an evaluation of catalytic performance.

Interaction between Metals and the Lignocellulose Supports. In a study on the synthesis of noble metal nanoparticles impregnated in cellulose paper,[23] He et al. concluded that the −OH and −C−O−C− functional groups in cellulose play an important chelating role as a "nanoparticle reactor". They proposed that ion−dipole interactions between the metal ions and cellulose oxygen-rich functional groups enabled the formation of very small (<10 nm) nanoparticles. This study also suggested that the nanoparticles were then stabilized by van der Waals forces with the cellulose, and did not observe any chemical bonding interactions between them. We did not observe chemical shifts in any ATR-FTIR spectra, suggesting that the Pd and Cu nanoparticles did not chemically bond to the supports. The XPS C(1s) envelopes for every catalyst showed no significant binding energy changes, supporting the same conclusion derived from ATR-FTIR. Consequently, our observations support those of He et al.,[23] and we conclude that the polar oxygen-containing functional groups (from cellulose within and at the surface of the milled fibers) serve as the sites for the metal atoms nucleation, reduction, and stabilization. We also postulate that these functional groups aid in creating colloid dispersions of the linen and bamboo during IW that result in the formation of well dispersed, small-sized metal nanoparticles.

Metal Loadings and Localization. Although ATR-FTIR and XPS data showed that the metals did not covalently bond to either support, a unique spatial distribution was observed for Pd and Cu within the fibers. XPS, TEM, and EDS results indicate that the Pd ions reduced to Pd metal preferentially in the near surface region (<ca. 500 nm) of the fibers, whereas Cu ions reduced to Cu metal more uniformly throughout the support. In EDS, as the acceleration voltage increased, an exponentially larger interaction volume of the fibers was probed by the SEM electron beam. The exponential decrease in Pd concentration observed from EDS measurements as acceleration voltage increased supports our conclusion that Pd was localized primarily on the fiber surfaces. Although this was observed for Pd in every catalyst, EDS measurements of Cu at each acceleration voltage were statistically similar and did not trend, indicating that Cu was more uniformly distributed throughout the support. These differences of metal nanoparticle localization occurred even though both metals were loaded in the fibers and reduced simultaneously.

In a related study of Pd−Cu catalysts prepared via IW of nitrate salts on pumice, Venezia et al. also reported disparities between measured and theoretical metal loadings in Pd−Cu bimetallic catalysts.[59] In that report, the authors proposed that Pd^{2+} reduced before Cu^{2+} on the pumice surface due to the higher redox potential of Pd^{2+}/Pd (0.915 V vs NHE) than Cu^{2+}/Cu (0.340 V vs NHE),[61] although Pd^{2+} and Cu^{2+} were coloaded onto the support using IW. We hypothesize that a similar phenomenon occurred on the lignocellulose Pd−Cu catalysts in our study.

DOI: 10.1021/acssuschemeng.6b01250
ACS Sustainable Chem. Eng. 2016, 4, 5511−5522

Although the trends in Pd and Cu localization on linen were similar to those on bamboo, the surface concentration Pd was higher on bamboo. This most likely resulted from, (i) higher O/C atomic ratio on the surface of milled bamboo fibers, indicating higher surface concentrations of cellulose after milling, and (ii) less uniform distribution of Pd^{2+} ions in bamboo fibers during IW caused by bamboo's higher hydrophobic lignin content.

Metal Nanoparticle Resistance to Oxidation. The Pd−Cu catalysts showed remarkable resistance to air oxidation at ambient conditions. XPS was performed more than 2 months after the catalysts were prepared and stored in air, yet the data showed that each remained primarily Pd and Cu metal, except for the sample with the highest Cu loading (L_5Pd10Cu). Cu is less noble than Pd, and its surface will oxidize during atmospheric exposure. However, alloys of Cu (e.g., brass) are more resistant to air oxidation. In separate studies, Venezia et al.[59] and Aduriz et al.[62] also observed Pd bimetal catalysts with high resistance to oxidation, and attributed it to the formation of Pd alloys. Each study used X-ray diffraction (XRD) to determine the presence and composition of the alloys. XRD analyses of our Pd−Cu catalysts did not yield well-resolved diffraction patterns, most likely due to the small nanoparticle size and interference from the crystalline support. However, SAED data collected from the TEM analyses of the catalysts did reveal that Pd−Cu alloys were formed, although the diffraction patterns were not precise enough to determine exact nanoparticle composition based on lattice parameters. Our TEM analysis determined that crystalline, metallic nanoparticles of heterogeneous composition formed throughout each lignocellulose matrix. The Pd−Cu alloy was predominantly observed only on the outside edges of both fibers, most likely because this is where Pd preferentially reduced and localized. Combined, the XPS and TEM data indicate that the oxidative stability of the catalyst was most likely due to the formation of a Pd−Cu alloy on the fiber surface.

Nitrite and Nitrate Reduction on Pd-Based Linen and Bamboo Powder Catalysts. For the linen-supported Pd catalysts, we hypothesize that increases in Pd loading led to a proportional increase of surface Pd sites and a corresponding increase in the rate of nitrite reduction, because each surface Pd site contributes equally for nitrite reduction for near-spherical Pd nanoparticles.[7] The linear relationship between nitrite reduction rate and Pd loading on linen catalysts suggests the reaction kinetics were not limited by hydrogen supply or aqueous/solid and intraparticle mass transfer (see the SI). For the bamboo-supported Pd catalysts, although nitrite reduction rate was not mass transfer limited (see the SI), it leveled off at Pd loadings beyond 3.8 wt %. The results could be explained by the higher Pd loadings on the surface of the bamboo fibers as determined by XPS. These higher surface Pd loadings may impact Pd nanoparticle surface area and therefore limit their catalytic performance.

For catalytic nitrate reduction, Pd−Cu catalysts on both supports exhibited an optimum Cu/(Cu+Pd) wt % for reactivity. Previous studies have reported the optimized Cu/(Cu+Pd) on other supports, including silica (20%),[46] pumice (23%),[63] alumina (33%),[45] and activated carbon (38%).[5] Our results are comparable with these previous studies; the most reactive Pd−Cu catalysts had an optimum Cu/(Cu+Pd) percentage of 34% and 41% on bamboo and linen, respectively. The existence of an optimum Cu loading indicates that Cu is an indispensable promoter for nitrate reduction, and that Pd−Cu interactions are critical to enhance the rate of nitrate reduction. A thorough kinetics study by Pintar et al. proposed that the mechanism for nitrate reduction in the Pd−Cu catalytic hydrogenation reaction involves heterolytic electron transfer between the active sites on Cu and Pd.[49] A study by Ilinitch et al. further highlighted the role of Cu metal as an oxygen scavenger in the reduction of nitrate to nitrite.[45] Sufficient Cu sites in close proximity or in direct contact with Pd are clearly necessary to promote catalytic nitrate reduction. Excessive amounts of Cu, however, likely reduce the number of accessible Pd surface sites, limiting hydrogen dissociation, a process required to regenerate zerovalent Cu and to reduce nitrate and other reaction intermediates (e.g., NO_2^-, N_2O).

Table S2 compares L_5Pd and L_5Pd3.3Cu with similar Pd and Pd−Cu catalysts loaded on conventional supports, and the performance of our lignocellulose-supported catalysts is comparable with those of conventional catalysts. Many studies have shown how initial catalyst loading, reaction pH and temperature, reagent concentrations, and support characteristics all impact nitrite/nitrate reduction rates.[2,47,64−66] Our reduction tests were conducted at a higher pH (7.3) in phosphate buffer (1 mM), and with lower initial contaminant concentration (0.1 mM), conditions which contributed to our lower observed reduction rates. The presence of a large amount of phosphate compared to nitrite/nitrate is expected to lower the reduction kinetics significantly, likely due to the competition between phosphate and nitrite/nitrate on catalyst surface.[67]

Creation of a Welded-Fiber Supported Pd−Cu Catalyst. In previous NFW applications of functional composites, active materials incorporated into the biopolymer matrix were premixed with cellulose binder and IL to create a suspension called the NFW "ink". A significant challenge was obtaining (and maintaining) a good suspension of the active material in the "ink". By incorporating catalytic metals directly into the lignocellulose powder, the cellulose binder and the active material required for the NFW "ink" were intimately integrated at the onset, and the resultant NFW "ink" stayed in suspension without difficulty. Thus, the processing methods developed in this study largely overcame this experimental challenge, significantly improving the NFW repertoire.

To develop a fiber-welded catalyst, the L_5Pd3.3Cu powder was first distributed in EMI-Ac and acetonitrile to form the NFW "ink". This solvent system effectively mobilizes cellulosic materials because of the chaotropic nature of the anion (acetate) and the hydrogen-bond basicity of the cation (imidazolium), which constitute the IL.[68] Acetonitrile is an effective molecular cosolvent with EMI-Ac, due to its strong hydrogen bond basicity that enhances cellulose dissolution.[69] While increasing the efficiency of cellulose mobilization, acetonitrile also reduces the "ink" viscosity for enhanced control in the NFW application.

The IL-based catalyst "ink" was deposited as a thin layer on the surface of the prewelded linen-scaffold shown in Figure 6. Exposure of the "ink" to the fibrous support was intentionally limited in order to control the dissolution of the prewelded linen-scaffold. Upon application, the IL-based solvent swelled the linen scaffold, mobilizing the biopolymers in the support to interact with and firmly anchor the catalyst powder. SEM and EDS mapping (Figure S8) revealed that the Pd−Cu catalyst remained on the outer surface of the natural fiber scaffold, and EDS measurements showed that the catalyst composition (Cu/(Cu+Pd)) was uniform.

DOI: 10.1021/acssuschemeng.6b01250
ACS Sustainable Chem. Eng. 2016, 4, 5511−5522

On the basis of previous experience developing NFW, we were confident the catalyst powder would effectively weld into the natural fiber support. It was less clear whether the IL solvent system might adversely affect catalytic activity. Acetate anion and acetonitrile were not expected to interact strongly with the Pd−Cu nanoparticles, and the imidazolium cation, with an extremely low acidic character should also be benign.[70] However, imidazolium cations can deprotonate at the C-2 position and form carbenes, highly reactive nucleophiles that can degrade the IL.[71,72] To mitigate this degradation, EMI-Ac is synthesized with a slight excess of acetic acid, whose moderate acidity could have compromised the catalyst. Our nitrate reduction tests indicate that exposing the catalysts to these IL solvent systems during NFW did not impact catalytic performance (Figure 7). These reactivity results also suggest that while serving as a robust support, the welded lignocellulose did not block the access of nitrate to the catalytic metals.

Although thorough characterization of the lignocellulose-supported Pd−Cu powders revealed nanoparticles with high oxidative stability over a two-month time frame, their catalytic performance declined during long-term storage in air at room temperature. Figure 5b shows the results for catalysts evaluated within 2 weeks of synthesis. In contrast, catalysts with the same composition, evaluated 2 months after they were prepared, exhibited a lower reactivity. Within 4 months of synthesis, the fiber-welded catalyst reactor had lost all reactivity (test 2 in Figure 7b). However, a simple tube furnace treatment at low temperature, conducted 8 months after the reactor had been originally fabricated and stored in air at room temperature, regenerated the welded-fiber catalyst (test 3 in Figure 7b) and restored its reactivity to a value expected for an L_5Pd3.3Cu catalyst (Figure 5b). During five subsequent 14-hour nitrate reduction tests, the system remained active and stable, showing no signs of deactivation during use (tests 4−8 Figure 7b). Stability during storage is therefore not a significant concern, considering (i) the catalyst's reactivity can easily be regenerated, and (ii) the catalyst should remain stable and reactive in practical nitrate reduction applications where it will be continuously exposed to the H_2 reducing agent.

Sustainability of the Lignocellulose Fiber Catalysts. NFW can produce many interesting functional composites. The advantage of using NFW to fabricate structures from natural fibers would be lost, however, if production came at a higher financial or environmental cost compared to traditional supports like activated carbon. We contend that the materials and processing methods used to create the presented systems offer a sustainable, cost-effective, and environmentally friendly alternative.

First, our nanoparticle fabrication process avoids the use of harsh chemicals or organic solvents and reduces the metals at low temperature, minimizing energy consumption and producing no hazardous waste. Although Pd is expensive, it is used at similar loadings for conventional supports (Table S2) to achieve comparable reactivity compared to our catalysts. Commercially available lignocellulose fibers require no further chemical modification and can be used as received. They are abundant, biodegradable, and can be fabricated into strong and robust composite materials with NFW. Furthermore, NFW employs nonvolatile, recyclable ILs to immobilize the nanomaterial into the support, with minimal leeching and without impacting catalytic performance. Moreover, NFW delivers a robust, free-standing structure of tunable, scalable size or shape that can easily be recovered and regenerated for subsequent use in contrast to many traditional supports. On the basis of the promising results from this study, we are actively developing these methods in order to design new materials with improved catalytic performance, robustness, and sustainability for water purification.

CONCLUSIONS

Lignocellulose yarns were used to support Pd and Pd−Cu nanoparticles for the catalytic hydrogenation of nitrate and nitrite. The processing methods were optimized to preserve the natural fibers, so the supported catalysts could be used in a natural fiber welding (NFW) application. Material characterization revealed that milling yarns into powder increased their surface area, exposing more oxygen-rich cellulose where metals preferentially bind. Linen fibers, with higher cellulose content than bamboo and more homogeneous cellulose distribution, supported a more reproducible metal loading and delivered catalysts with slightly increased reactivity for nitrite and nitrate reduction. A low temperature, hydrogen gas reduction process reduced Pd and Cu to their zerovalent (elemental) state, although no specific chemical bonding was observed between the metals and their supports. A unique spatial distribution of metals was observed in all bimetal catalysts, with Pd and Pd−Cu accumulation on the surface and uniform distribution of Cu through the bulk. TEM of Pd and Pd−Cu catalysts revealed the formation of crystalline, near-spherical, metallic nanoparticles (ca. 5−10 nm), including Pd−Cu alloy on the fiber surfaces. Nitrite and nitrate reduction kinetics were investigated for each catalyst, and an optimized Cu loading for nitrate reduction was found for Pd−Cu catalysts supported on linen and bamboo.

Through NFW, the linen-supported Pd−Cu nanoparticles were immobilized on the surface of an all-lignocellulose matrix using an IL-based solvent that did not degrade catalyst performance. A rigorous evaluation of the fiber-welded Pd−Cu catalyst demonstrated its catalytic stability, reusability, and sustainability toward the reduction of nitrate. This novel study presents a scalable method of incorporating catalytic nanomaterials into lignocellulose matrices to design robust, portable, free-standing sustainable catalysts for water purification that could be less expensive and more versatile than current catalyst supports. Moreover, these methods extend well beyond the current water treatment application. Given the vast number of cellulose-based materials to which NFW can be applied, and the many options for functional nanomaterials, our study demonstrates a simple, low-cost, and sustainable method to generate a wide variety of advanced functional materials.

ASSOCIATED CONTENT

Supporting Information

The Supporting Information is available free of charge on the ACS Publications website at DOI: 10.1021/acssuschemeng.6b01250.

Elemental analyses (XPS and EDS) of bamboo supported Pd-based catalysts (Figures S1−3), ATR-FTIR analyses of linen and bamboo Pd-based catalysts (Figure S4), XPS spectra of linen and bamboo catalysts (Figures S5−6), TEM/EDS analyses of linen and bamboo catalysts (Figure S7), SEM/EDS analysis of fiber-welded catalyst (Figure S8), ICP-MS analyses of linen and bamboo Pd-based catalysts (Table S1), comparison of catalyst performance (Table S2) (PDF)

DOI: 10.1021/acssuschemeng.6b01250
ACS Sustainable Chem. Eng. 2016, 4, 5511−5522

AUTHOR INFORMATION

Corresponding Author

*D. Shuai. Phone: 202-994-0506. Email: danmengshuai@gwu.edu.

Notes

The authors declare no competing financial interest.

ACKNOWLEDGMENTS

We acknowledge startup funds from the Department of Civil and Environmental Engineering, The George Washington University (GW), and the Johns Hopkins University Water SEED grant. We thank Nathan A. Banek and Prof. Michael J. Wagner of the Department of Chemistry, GW, for liquid N_2 adsorption measurements. We are grateful to the Air Force Office of Scientific Research for funding, and Johns Hopkins University and the U.S. Naval Academy for facilities support. Any opinions, findings and conclusions, or recommendations expressed in this paper are those of the authors and do not reflect the views of the U.S. Air Force or the U.S. Navy.

REFERENCES

(1) Batista, J.; Pintar, A.; Ceh, M. Characterization of supported Pd-Cu bimetallic catalysts by SEM, EDXS, AES and catalytic selectivity measurements. *Catal. Lett.* **1997**, *43*, 79−84.

(2) Wada, K.; Hirata, T.; Hosokawa, S.; Iwamoto, S.; Inoue, M. Effect of supports on Pd−Cu bimetallic catalysts for nitrate and nitrite reduction in water. *Catal. Today* **2012**, *185*, 81−87.

(3) Verma, S.; Nandi, M.; Modak, A.; Jain, S. L.; Bhaumik, A. Novel organic-inorganic hybrid mesoporous silica supported oxo-vanadium schiff base for selective oxidation of alcohols. *Adv. Synth. Catal.* **2011**, *353* (11−12), 1897−1902.

(4) Kim, M.; Chung, S.; Yoo, C.; Lee, M.; Cho, I.; Lee, D.; Lee, K. Catalytic reduction of nitrate in water over Pd−Cu/TiO_2 catalyst: effect of the strong metal-support interaction (SMSI) on the catalytic activity. *Appl. Catal., B* **2013**, *142−143*, 354−361.

(5) Soares, O.; Orfao, J.; Pereira, M. Bimetallic catalysts supported on activated carbon for the nitrate reduction in water: optimization of catalysts composition. *Appl. Catal., B* **2009**, *91*, 441−448.

(6) Verma, S.; Kumar, S.; Shawat, E.; Nessim, G. D.; Jain, S. L. Carbon nanofibers decorated with oxo−rhenium complexes: Highly efficient heterogeneous catalyst for oxidation of amines with hydrogen peroxide. *J. Mol. Catal. A: Chem.* **2015**, *402*, 46−52.

(7) Shuai, D.; Choe, J. K.; Shapley, J. R.; Werth, C. J. Enhanced activity and selectivity of carbon nanofiber supported Pd catalysts for nitrite reduction. *Environ. Sci. Technol.* **2012**, *46*, 2847−2855.

(8) Huang, Y.; Miao, Y.; Ji, S.; Tjiu, W. W.; Liu, T. Electrospun carbon nanofibers decorated with Ag−Pt bimetallic nanoparticles for selective detection of dopamine. *ACS Appl. Mater. Interfaces* **2014**, *6*, 12449−12456.

(9) Hull, R. V.; Li, L.; Xing, Y. C.; Chusuei, C. C. Pt nanoparticle binding on functionalized multiwalled carbon nanotubes. *Chem. Mater.* **2006**, *18* (7), 1780−1788.

(10) Verma, S.; Nasir Baig, R. B.; Nadagouda, M. N.; Varma, R. S. Visible light mediated upgrading of biomass to biofuel. *Green Chem.* **2016**, *18* (5), 1327−1331.

(11) Baig, R. B. N.; Verma, S.; Varma, R. S.; Nadagouda, M. N. Magnetic Fe@g-C_3N_4: a photoactive catalyst for the hydrogenation of alkenes and alkynes. *ACS Sustainable Chem. Eng.* **2016**, *4* (3), 1661−1664.

(12) Bayer, P.; Heuer, E.; Karl, U.; Finkel, M. Economical and ecological comparison of granular activated carbon (GAC) adsorber refill strategies. *Water Res.* **2005**, *39*, 1719−1728.

(13) Hjaila, K.; Baccar, R.; Sarra, M.; Gasol, C. M.; Blanquez, P. Environmental impact associated with activated carbon preparation from olive-waste cake via life cycle assessment. *J. Environ. Manage.* **2013**, *130*, 242−247.

(14) Lewin, M. *Handbook of Fiber Chemistry*, 3rd ed.; CRC Press, Taylor and Francis Group, LLC: Boca Raton, FL, 2007.

(15) Freudenberg, K.; Nash, N. C. *Constitution and biosynthesis of lignin*. Springer-Verlag: Berlin, 1968.

(16) Needles, H. L. *Textile fibers, dyes, finishes, and processes*; Noyes Publications: Park Ridge, NJ, 1986.

(17) John, M.; Anandjiwala, R. Recent developments in chemical modification and characterization of natural fiber-reinforced composites. *Polym. Compos.* **2008**, *29*, 187−207.

(18) Dorez, G.; Ferry, L.; Sonnier, R.; Taguet, A.; Lopez-Cuesta, J. Effect of cellulose, hemicellulose and lignin contents on pyrolysis and combustion of natural fibers. *J. Anal. Appl. Pyrolysis* **2014**, *107*, 323−331.

(19) Liese, W.; Kohl, M. *Bamboo: the plant and its uses*; Springer International Publishing: Switzerland, 2015.

(20) Gani, A.; Naruse, I. Effect of cellulose and lignin content on pyrolysis and combustion characteristics for several types of biomass. *Renewable Energy* **2007**, *32*, 649−661.

(21) Shen, D.; Xiao, R.; Gu, S.; Zhang, H. The overview of thermal decomposition of cellulose in lignocellulosic biomass. In *Cellulose - Biomass Conversion*; van de Ven, T., Kadla, J., Eds.; InTech: Rijeka, Croatia, 2013; pp 1−34, DOI: 10.5772/51883.

(22) Quignard, F.; Choplin, A. Cellulose: a new bio-support for aqueous phase catalysts. *Chem. Commun.* **2000**, *2001*, 21−22.

(23) He, J.; Kunitake, T.; Nakao, A. Facile in situ synthesis of noble metal nanoparticles in porous cellulose fibers. *Chem. Mater.* **2003**, *15*, 4401−4406.

(24) Reddy, K.; Kumar, N.; Reddy, P.; Sreedhar, B.; Kantam, M. Cellulose supported palladium (0) catalyst for heck and sonogashira coupling reactions. *J. Mol. Catal. A: Chem.* **2006**, *252*, 12−16.

(25) Padalkar, S.; Capadona, J.; Rowan, S.; Weder, C.; Won, Y.; Stanciu, L.; Moon, R. Natural biopolymers: novel templates for the synthesis of nanostructures. *Langmuir* **2010**, *26* (11), 8497−8502.

(26) Haverhals, L. M.; Reichert, W. M.; De Long, H. C.; Trulove, P. C. Natural fiber welding. *Macromol. Mater. Eng.* **2010**, *295* (5), 425−430.

(27) Haverhals, L. M.; Nevin, L. M.; Foley, M. P.; Brown, E. K.; De Long, H. C.; Trulove, P. C. Fluorescence monitoring of ionic liquid-facilitated biopolymer mobilization and reorganization. *Chem. Commun.* **2012**, *48*, 6417−6419.

(28) Hulsbosch, J.; De Vos, D. E.; Binnemans, K.; Ameloot, R. Biobased ionic liquids: solvents for a green processing industry? *ACS Sustainable Chem. Eng.* **2016**, *4* (6), 2917−2931.

(29) Haverhals, L. M.; Sulpizio, H. M.; Fayos, Z. A.; Trulove, M. A.; Reichert, W. M.; Foley, M. P.; De Long, H. C.; Trulove, P. C. Process variables that control natural fiber welding: time, temperature, and amount of ionic liquid. *Cellulose* **2012**, *19* (1), 13−22.

(30) Haverhals, L. M.; Sulpizio, H. M.; Fayos, Z. A.; Trulove, M. A.; Reichert, W. M.; Foley, M. P.; De Long, H. C.; Trulove, P. C. Process variables that control natural fiber welding. *ECS Trans.* **2010**, *33* (7), 79−90.

(31) Haverhals, L. M.; Isaacs, T. A.; Page, E. C.; Reichert, W. M.; De Long, H. C.; Trulove, P. C. Ionic liquids in the preparation of biopolymer composite materials. *Electrochem. Soc. Trans.* **2008**, *16* (49), 129−139.

(32) Haverhals, L. M.; Sulpizio, H. M.; Fayos, Z. A.; Trulove, M. A.; Reichert, W. M.; Foley, M. P.; De Long, H. C.; Trulove, P. C. Characterization of polymer movement in fiber welded cellulose composites. *ECS Trans.* **2010**, *33* (7), 91−98.

(33) Jost, K.; Durkin, D. P.; Haverhals, L. M.; Brown, E. K.; Langenstein, M.; De Long, H. C.; Trulove, P. C.; Gogotsi, Y.; Dion, G. Natural fiber welded electrode yarns for knittable textile supercapacitors. *Adv. Funct. Mater.* **2015**, *5*, 1−8.

(34) Burow, K. R.; Nolan, B. T.; Rupert, M. G.; Dubrovsky, N. M. Nitrate in groundwater of the United States, 1991−2003. *Environ. Sci. Technol.* **2010**, *44*, 4988−4997.

(35) Spalding, R. F.; Exner, M. E. Occurence of nitrate in groundwater - a review. *J. Environ. Qual.* **1993**, *22*, 392−402.

DOI: 10.1021/acssuschemeng.6b01250
ACS Sustainable Chem. Eng. 2016, 4, 5511−5522

(36) Wakida, F. T.; Lerner, D. N. Non-agricultural sources of groundwater nitrate: a review and case study. *Water Res.* **2005**, *39*, 3−16.
(37) Degnan, J. R.; Bohlke, J. K.; Pelham, K.; Langlais, D. M.; Walsh, G. J. Identification of groundwater nitrate contamination from explosives used in road construction: isotopic, chemical, and hydrologic evidence. *Environ. Sci. Technol.* **2016**, *50* (2), 593−603.
(38) Fewtrell, L. Drinking-water nitrate, methemoglobinemia, and global burden of disease: a discussion. *Environ. Health Perspect.* **2004**, *112* (14), 1371−1374.
(39) Mirvish, S. S. Gastric cancer and salivary nitrate and nitrite. *Nature* **1985**, *315*, 461−462.
(40) Weyer, P. J.; Cerhan, J. R.; Kross, B. C.; Hallberg, G. R.; Kantamneni, J.; Breuer, G.; Jones, M. P.; Zheng, W.; Lynch, C. F. Municipal drinking water nitrate level and cancer risk in older women: the Iowa women's health study. *Epidemiology* **2001**, *11*, 327−338.
(41) WHO. *Guidelines for drinking-water quality*; World Health Organization: Geneva, 2008.
(42) USEPA. *National primary drinking water regulations*; U.S. Government Printing Office: Washington DC, 2010.
(43) Prusse, U.; Hahnlein, M.; Daum, J.; Vorlop, K. D. Improving the catalytic nitrate reduction. *Catal. Today* **2000**, *55*, 79−90.
(44) Yoshinaga, Y.; Akita, T.; Mikami, I.; Okuhara, T. Hydrogenation of nitrate in water to nitrogen over Pd-Cu supported on active carbon. *J. Catal.* **2002**, *207*, 37−45.
(45) Ilinitch, O. M.; Nosova, L. V.; Gorodetskii, V. V.; Ivanov, V. P.; Trukhan, S. N.; Gribov, E. N.; Bogdanov, S. V.; Cuperus, F. P. Catalytic reduction of nitrate and nitrite ions by hydrogen: investigation of the reaction mechanism over Pd and Pd-Cu catalysts. *J. Mol. Catal. A: Chem.* **2000**, *158*, 237−249.
(46) Horold, S.; Vorlop, K. D.; Tacke, T.; Sell, M. Development of catalysts for a selective nitrate and nitrite removal from drinking water. *Catal. Today* **1993**, *17*, 21−30.
(47) Prusse, U.; Vorlop, K. Supported bimetallic palladium catalysts for water-phase nitrate reduction. *J. Mol. Catal. A: Chem.* **2001**, *173*, 313−328.
(48) Gauthard, F.; Epron, F.; Barbier, J. Palladium and platinum-based catalysts in the catalytic reduction of nitrate in water: effect of copper, silver, or gold addition. *J. Catal.* **2003**, *220* (1), 182−191.
(49) Pintar, A.; Batista, J.; Levec, J.; Kajiuchi, T. Kinetics of the catalytic liquid-phase hydrogenation of aqueous nitrate solutions. *Appl. Catal., B* **1996**, *11* (1), 81−98.
(50) Pintar, A.; Bercic, G.; Levec, J. Catalytic liquid-phase nitrite reduction: kinetics and catalyst deactivation. *AIChE J.* **1998**, *44* (10), 2280−2292.
(51) Bausells, J. *Electron interaction with solids - single scattering monte carlo simulation software*, 3.0; Barcelona, Spain, 2008.
(52) Liu, Y. Recent Progress in Fourier Transform Infrared (FTIR) Spectroscopy Study of Compositional, Structural and Physical Attributes of Developmental Cotton Fibers. *Materials* **2013**, *6*, 299−313.
(53) Moulder, J. F.; Stickle, W. F.; Sobol, P. E.; Bomben, K. D. *Handbook for X-Ray Photoelectron Spectroscopy*; Physical Electronics Inc.: Chanhassen, MN, 1995.
(54) Batista, J.; Pintar, A.; Mandrino, D.; Jenko, M.; Martin, V. XPS and TPR examinations of g-alumina supported Pd-Cu catalysts. *Appl. Catal., A* **2001**, *206*, 113−124.
(55) Speckmann, H. D.; Haupt, S.; Strehblow, H. A quantitative surface analytical study of electrochemically-formed copper oxides by XPS and x-ray-induced auger spectroscopy. *Surf. Interface Anal.* **1988**, *11*, 148−155.
(56) Csiszar, E.; Fekete, E. Microstructure and surface properties of fibrous and ground cellulosic substrates. *Langmuir* **2011**, *27*, 8444−8450.
(57) Allemand, M.; Martin, M.; Reyter, D.; Roue, L.; Guay, D.; Andrei, C.; Botton, G. Synthesis of Cu−Pd alloy thin films by co-electrodeposition. *Electrochim. Acta* **2011**, *56*, 7397−7403.
(58) Meshesha, B. T.; Barrabes, N.; Llorca, J.; Dafinov, A.; Medina, F.; Fottinger, K. PdCu alloy nanoparticles on alumina as selective catalysts for trichloroethylene hydrodechlorination to ethylene. *Appl. Catal., A* **2013**, *453*, 130−141.
(59) Venezia, A. M.; Liotta, L. F.; Deganello, G.; Schay, Z.; Guczi, L. Characterization of pumice-supported Ag−Pd and Cu−Pd bimetallic catalysts by x-ray photoelectron spectroscopy and x-ray diffraction. *J. Catal.* **1999**, *182*, 449−455.
(60) Rutkowski, P. Catalytic effects of copper(II) chloride and aluminum chloride on the pyrolytic behavior of cellulose. *J. Anal. Appl. Pyrolysis* **2012**, *98*, 86−97.
(61) Bard, A. J.; Faulkner, L. R. *Electrochemical methods, fundamentals and applications*, 2nd ed.; John Wiley & Sons, Ltd: Hoboken, NJ, 2001.
(62) Aduriz, H. R.; Bodnariuk, P.; Coq, B.; Figueras, F. Alumina-supported bimetallics of palladium alloyed with germanium, lead, or antimony from organometallic precursors: preparation and characterization. *J. Catal.* **1989**, *119* (1), 97−107.
(63) Deganello, F.; Liotta, L.; Macaluso, A.; Venezia, A.; Deganello, G. Catalytic reduction of nitrates and nitrites in water solution on pumice-supported Pd-Cu catalysts. *Appl. Catal., B* **2000**, *24* (3−4), 265−273.
(64) Gao, W.; Guan, N.; Chen, J.; Guan, X.; Jin, R.; Zeng, H.; Liu, Z.; Zhang, F. Titania supported Pd-Cu bimetallic catalyst for the reduction of nitrate in drinking water. *Appl. Catal., B* **2003**, *46*, 341−351.
(65) Palomares, A. E.; Prato, J. G.; Márquez, F.; Corma, A. Denitrification of natural water on supported Pd/Cu catalysts. *Appl. Catal., B* **2003**, *41* (1−2), 3−13.
(66) Soares, O.; Orfao, J.; Pereira, M. Activated carbon supported metal catalysts for nitrate and nitrite reduction in water. *Catal. Lett.* **2008**, *126*, 253−260.
(67) Ye, T.; Durkin, D. P.; Hu, M.; Wang, X.; Banek, N.; Wagner, M.; Shuai, D. Enhancement of nitrite reduction kinetics on electrospun Pd-carbon nanomaterial catalysts for water purification. *ACS Appl. Mater. Interfaces* **2016**, *8* (28), 17739−17744.
(68) Rinaldi, R. Instantaneous dissolution of cellulose in organic electrolyte solutions. *Chem. Commun.* **2011**, *47*, 511−513.
(69) Kamlet, M. J.; Abboud, J. L. M.; Abraham, M. H.; Taft, R. W. Linear solvation energy relationships. A comprehensive collection of solvatochromic parameters, p*, a, and b, and some methods for simplifying the generalized solvatochromic equation. *J. Org. Chem.* **1983**, *48*, 2877−2887.
(70) Amyes, T. L.; Diver, S. T.; Richard, J. P.; Rivas, F. M.; Toth, K. Formation and stability of N-heterocyclic carbenes in water: the carbon acid pKa of imidazolium cations in aqueous solution. *J. Am. Chem. Soc.* **2004**, *126* (13), 4366−4374.
(71) Wasserscheid, P.; Welton, T. *Ionic liquids in synthesis*; Wiley-VCH: Germany, 2008.
(72) Holloczki, O.; Gerhard, D.; Massone, K.; Szarvas, L.; Nemeth, B.; Veszpremi, T.; Nyulaszi, L. Carbenes in ionic liquids. *New J. Chem.* **2010**, *34*, 3004−3009.

DOI: 10.1021/acssuschemeng.6b01250
ACS Sustainable Chem. Eng. 2016, 4, 5511−5522